J SYST SCI SYST ENG
Vol. 30, No. 5, October 2021, pp. 626–646
DOI: https://doi.org/10.1007/s11518-021-5506-4
ISSN: 1004-3756 (paper), 1861-9576 (online)
CN 11-2983/N

Agile Earth Observation Satellite Scheduling Algorithm for Emergency Tasks Based on Multiple Strategies

Haiquan Sun, Wei Xia, Zhilong Wang, Xiaoxuan Hu

[a]School of Management, Hefei University of Technology, Hefei, China
[b]Key Laboratory of Process Optimization and Intelligent Decision-making, Ministry of Education, Hefei, China
sunhaiquan2015@163.com, xiawei@hfut.edu.cn, wangzhilong@mail.hfut.edu.cn, xiaoxuanhu@hfut.edu.cn (✉)

Abstract. During the execution of imaging tasks, satellites are often required to observe natural disasters, local wars, and other emergencies, which regularly interferes with the execution of existing schemes. Thus, rapid satellite scheduling is urgently needed. As a new generation of three degree-of-freedom (roll, pitch, and yaw) satellites, agile earth observation satellites (AEOSs) have longer variable-pitch visible time windows for ground targets and are capable of observing at any time within the time windows. Thus, they are very suitable for emergency tasks. However, current task scheduling models and algorithms ignore the time, storage and energy consumed by pitch. Thus, these cannot make full use of the AEOS capabilities to optimize the scheduling for emergency tasks. In this study, we present a fine scheduling model and algorithm to realize the AEOS scheduling for emergency tasks. First, a novel time window division method is proposed to convert a variable-pitch visible time window to multiple fixed-pitch visible time windows. Second, a model that considers flexible pitch and roll capabilities is designed. Finally, a scheduling algorithm based on merging insertion, direct insertion, shifting insertion, deleting insertion, and reinsertion strategies is proposed to solve conflicting problems quickly. To verify the effectiveness of the algorithm, 48 groups of comparative experiments are carried out. The experimental results show that the model and algorithm can improve the emergency task completion efficiency of AEOSs and reduce the disturbance measure of the scheme. Furthermore, the proposed method can support hybrid satellite resource scheduling for emergency tasks.

Keywords: Agile earth observation satellites, emergency tasks, merging insertion, shifting insertion

1. Introduction

Earth observation satellites (EOSs) are objects around the earth that use remote sensors to obtain ground image information (Cordeau et al. 2005). They play increasingly important roles in military, industrial, and agricultural fields due to their various advantages, such as wide coverage ranges and borderless limitations (Li et al. 2017). In particular, EOSs have become important tools to obtain first-hand information during emergency Earth observations. For example, when an earthquake occurs, the images of the disaster area are acquired by EOSs. The observation is expected to be acquired within tens of seconds or even seconds to carry out the disaster assessment and formulate a rescue plan in time. The new generation EOSs, agile EOSs (AEOSs), have three degrees of freedom (roll, pitch, and yaw), unlike conventional EOSs (CEOSs). This enables the AEOSs to observe targets before or after flying above them. As shown in Figure 1, this agility greatly enhances the observation opportunities for emergency tasks as well as the system response speed and robustness. Thus, this kind of flexible satellite is highly suitable for emergency task observation.

Although AEOSs have higher emergency observation potential, AEOS scheduling is more difficult than CEOS scheduling, which is mainly because of the more complicated models and larger solution space. Due to the pitch-

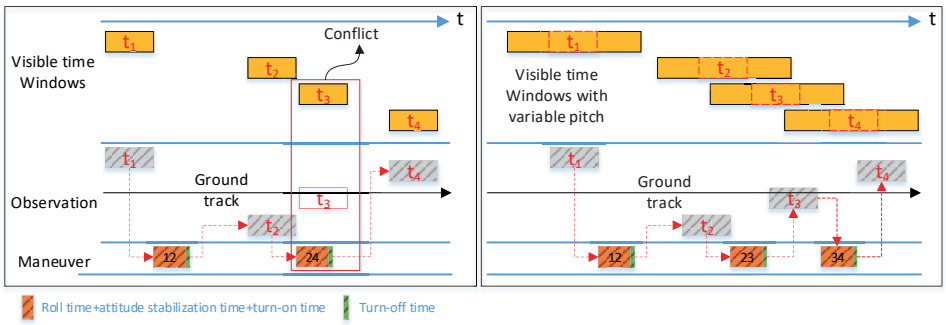

Figure 1 Schemes of CEOSs (Left) and AEOSs (Right)[1]

ing capabilities of AEOSs, the variable-pitch visible time window (VPVTW) is much longer than the required time of the task. Theoretically, the observation duration can be anywhere within the VPVTW as long as it does not conflict with the other tasks. The number of possible observation times simultaneously increases dramatically. Hence, the high freedom for the VPVTW and start time selection increases the problem complexity. AEOSs also have the ability to roll sideways, which leads to time dependence of the scheme. The transition time between two consecutive observations is related to the observations, as the start time of the next observation depends on the end time of the previous observation. When the interval between the two tasks cannot meet the time of the maneuver, including the roll, attitude stabilization, turn-on, and turn-off times for the waiting task, the maneuver operations for the tasks before the waiting task can be adjusted appropriately to reduce the maneuver time. As shown in Figure 1, task 3 can be inserted by adjusting the maneuver operation for task 2, such that maneuver 24 becomes maneuvers 23 and 34. This dramatically increases the possibility of task insertion and increases the size of the solution space of the scheduling problem. In addition, emergency tasks often have short deadlines and high values (Niu et al. 2015). If they cannot be finished within a given period or deadline, the observation may be useless for users (Zhu et al. 2017), which increases the complexity of a scheduling problem. In view of this, the AEOS scheduling problem for emergency tasks urgently needs a novel and effective model and algorithm.

Most previous researches focus on AEOS scheduling for general tasks (Xie et al. 2019, Li and Li 2019, Liu et al. 2017, He et al. 2018) and CEOS scheduling for emergency tasks (Sun et al. 2019, Niu et al. 2018, Liu and Hodgson 2016), but there are few researches on AEOS scheduling for emergency tasks. With the rapid increase in user demand, when the emergency tasks arrive, there may be a large number of scheduled tasks in the scheme. The previous scheduling algorithms have difficulty dealing with this issue quickly and effectively. The reasons are as follows. (i) In previous scheduling algorithms, the resource objects are not AEOSs, or the scheduling constraints of the AEOSs are simplified. For example, the pitch capability increases the length of the observation time window. However, the time, storage and energy consumed by the pitch maneuver are not considered, which may result in a deviation of the scheduling scheme from the actual demand. Thus, a more accurate model is required. (ii) At present, the AEOS load is often nearly full. In this case, it is difficult to find idle times for emergency tasks, which creates an over-ordering problem. This places higher requirements on the capabilities of the optimization algorithm. (iii) AEOSs have such flexible pitch and roll capabilities that they have longer VPVTWs for emergency tasks before the completion deadline. The determination of

the observation start time has a strong dependence on the observation angle of the scheduled scheme, which increases the complexity of the emergency task scheduling problem.

For such problems, we develop a novel time window division method to convert a VPVTW to multiple fixed-pitch visible time windows(VTWs). We then design a more accurate model of AEOS scheduling for emergency tasks. In addition to the general limitations of the data transmission time, on-off time, storage, and energy (Baek et al. 2011), we also consider the limitations of the roll, pitch, and attitude stabilization times for AEOSs and the completion times for emergency tasks. To solve this model, we propose a novel merging insertion, direct insertion, shifting insertion, deleting insertion, and reinsertion strategy (MISDR) algorithm with two heuristic factors. Based on the pitch and roll capabilities of AEOSs, we design a task merging strategy. In this strategy, similar tasks are included in the same observation strip, which can increase the flexibility of the task time window selection and reduce the turn-on, turn-off, roll, and attitude stability times of AEOSs. It is beneficial to conserve the AEOS resources and promote the scheduling probability of the task. Based on the fact that a VTW is longer than the task observation time, the task shifting strategy is designed. Under satisfying the observation constraints, the conflicting tasks can be moved forward or backward within their own VTWs, which can improve the insertion possibility of emergency tasks. In addition, we design two heuristic factors, the urgency degree of an emergency task and the merging degree of a time window, to guide the task insertion sequence and task merging time window selection.

To verify the effectiveness and scalability of the model and algorithm, we design an AEOS and a hybrid satellite resource scheduling scenarios for emergency tasks and compare the performance of the proposed algorithm with the direct insertion, shifting insertion, deleting insertion, and reinsertion (ISDR) algorithm (Wang et al. 2014) as well as a dynamic emergency scheduling with task merging, backward shift and rehabilitation (TMBSR-DES) algorithm (Wang et al. 2014). The experimental results verify that the proposed MISDR algorithm can improve the task completion efficiency and reduce the disturbance measure of the scheme. Accordingly, the designed model and algorithm can effectively address the AEOS scheduling problem for emergency tasks and support hybrid satellite resource scheduling for emergency tasks.

The remainder of this paper is organized as follows. Related work is surveyed in Section 2. In Section 3, an overview of the rescheduling problem is provided. In Section 4, we present a time window division method and an AEOS scheduling model for emergency tasks. We introduce the corresponding solution, which includes the MISDR algorithm and two heuristic factors in Section 5. The simulation experiments and performance analysis are given in Section 6. Finally, in Section 7, the paper is concluded, and future work is discussed.

2. Related Work

In the process of carrying out tasks, EOSs inevitably encounter some emergency tasks, such as natural disasters, local wars, etc. Due to the high value and time sensitivity of such tasks, it is urgent to adjust the original schemes of EOSs quickly (Zhai et al. 2015). Simultaneously, EOSs can be classified into CEOSs and AEOSs based on maneuverability (He et al. 2018). Therefore, the previous researches in this field mainly focus on CEOS scheduling problem and AEOS scheduling problem for emergency tasks.

Due to the early appearance of CEOSs, there are many researches on the CEOS scheduling problem for emergency tasks, and its scheduling algorithms mainly include

meta-heuristic and heuristic algorithms. Wu et al. (2012) proposed a pretreatment process to eliminate conflicts between emergency tasks and allocate all tasks to the related CEOS orbits. Thereafter, a mathematical model and a directed acyclic graph model were constructed. Finally, a hybrid ant colony optimization method combined with an iterative local search was established to solve the CEOS scheduling problem for emergency and general tasks. Zhai et al. (2015) proposed the HA-NSGA2 dynamic scheduling algorithm to maximize the schedule benefits and robustness in which a non-dominated sorting genetic algorithm and rule-based heuristic algorithm were combined. Because the response time and stability of solutions with meta-heuristic algorithms are relatively poor, it may be difficult to complete the scheduling before the time required by users. For this reason, Based on the characteristics of emergency tasks with independent arrival times and task completion deadlines, Qiu et al. (2013) combined the rolling horizon strategy with a heuristic algorithm to form a dynamic scheduling algorithm for emergency tasks, which improved the CEOS scheduling efficiency. Wang et al. (2014) designed two heuristic algorithms to solve the CEOS scheduling problem after analyzing the dynamic properties of CEOS scheduling. The first heuristic algorithm arranged new tasks by insertion or deletion and then inserted tasks repeatedly based on their priority from low to high. The second algorithm adopted four steps: insert directly, insert by shifting, insert by deletion, and reinsert the deleted tasks. The two algorithms were compared in terms of efficiency and response time.

Due to the poor flexibility of the CEOSs, the VTWs of CEOSs are much shorter than those of AEOSs, and even they are selected as the observation time window directly in the previous researches. However, with the increase in the number and the required response speed of emergency tasks, the possibility of inserting emergency tasks into the scheme is lower. Therefore, CEOS service capabilities have been stretched to their flexibility limits.

With the development of satellite capabilities, AEOSs, new generation EOSs with three degrees of freedom, have longer visible time windows and more flexible pitch and roll operation for targets, which can create more possibilities to insert tasks in the scheduling scheme. Thus, AEOSs are highly suitable for the scheduling for emergency tasks. However, to the best of our knowledge, most previous researches focus on AEOS scheduling for general tasks, the corresponding scheduling algorithms mainly include the genetic algorithm (Wang et al. 2019), ant colony algorithm (Du et al. 2018, Cui et al. 2018), tabu search algorithm (Habet et al. 2010), greedy algorithm (Lemaître et al. 2002) and constructive heuristic algorithm (Wang et al. 2011, BunChenkheila et al. 2016, He et al. 2019). There are few researches on AEOS scheduling for emergency tasks. Guo et al. (2012) proposed a heuristic-based scheme adjustment method for AEOSs to adjust the original scheme and add newly arrived, urgent observations into the scheme dynamically, and three heuristic rules are given to improve the performance of the algorithm. Given the difficulty of predicting environmental uncertainties, He et al. (2019) proposed a hierarchical scheduling method based on the ant colony algorithm for the real-time scheduling problem. This method can effectively reduce the impact of unexpected environmental changes and obtain a higher solution profit.

In the above algorithms, the resource objects are not AEOSs, or the scheduling constraints of the AEOSs are simplified. For example, the pitch capability only increases the length of the observation time window. However, the time, storage and energy consumed by the pitch maneuver are not considered, which

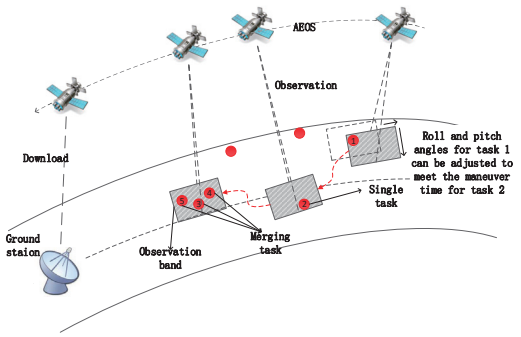

Figure 2 Observation Process of AEOSs

may result in a deviation of the scheduling scheme from the actual demand. Although AEOSs have such flexible pitch and roll capabilities that they have longer VPVTWs for emergency tasks before the completion deadline, there is no specific optimization strategy designed for pitch and roll capabilities, and the VPVTWs are not divided reasonably, even directly used without considering the pitch angle. Simultaneously, with the rapid increase of tasks, the AEOS load is often nearly full in actual applications. In this case, it is difficult to find idle times for emergency tasks.

In this paper, we first develop a novel time window division method including a discrete granularity and division rule, which can convert a VPVTW to multiple VTWs. We then comprehensively consider the characteristics of the agile satellite pitch and roll capabilities and the completion deadline of emergency tasks to design a model suitable for AEOS scheduling for emergency tasks. We finally propose a novel MISDR algorithm to complete AEOS scheduling for emergency tasks. In this algorithm, the merging insertion strategy is designed for the AEOS's pitch and roll capabilities, by which tasks with similar distances are included in the same observation strip. The shifting insertion strategy is designed for the long VTWs, by which the conflicting tasks can be moved forward and backward in a long VTW to complete task insertion. Therefore, the task completion efficiency of AEOSs and the disturbance measure of the scheme are expected to be improved.

Table 1 The Table of Abbreviations

Abbreviation	Description
EOS	Earth observation satellite
AEOS	Agile earth observation satellite
CEOS	Conventional earth observation satellite
VPVTW	Variable-pitch visible time window
VTW	Fixed-pitch visible time window
OTW	Observation time window

3. Problem Description

AEOSs in orbit observe ground targets through remote sensors. The remote sensor has a specific field of view. As shown in Figure 2, each observation action will form a band with a certain width and length on the ground. The ground targets studied in this paper are point targets, that is, during the observation process, a ground target only needs to be observed once. When the time interval between adjacent tasks cannot meet the maneuver time requirements, the roll and pitch angles of the tasks can be adjusted appropriately to reduce the time. Of course, when the intervals between multiple adjacent tasks cannot meet the maneuver time requirements and they are closer to each other, they can be included in the same observation band for observation by adjusting the roll angle, i.e., observing at the same time with other tasks. The data obtained from each observation will be temporarily stored in the AEOS's memory. When the AEOS storage reaches full capacity, the data must be downloaded to the ground station before the next observation (Bianchessi et al. 2007). The observation, maneuver, and downloading operations will consume a certain amount of energy. The AEOS energy is limited within each orbit circle, and the consumption cannot exceed the maximum energy. The research of this paper is to insert emergency tasks into the original schemes without violating these constraints and maximize the value of the new scheme.

For understanding the meaning of abbreviations conveniently in this paper, a table of

abbreviations is listed in Table 1.

3.1 Problem Analysis

The problem studied in this paper not only includes the general limitations of the data transmission time, on-off time, storage, and energy, but also includes the limitations of the roll, pitch, and attitude stabilization times for AEOSs and the completion times for emergency tasks. Simultaneously, in order to give full play to AEOS's flexible pitch and roll capacities to complete the emergency tasks with a short deadline and high value, the way of observing multiple tasks at one time is allowed in this study. These make the problem more in line with the actual application process of AEOSs. Since the scheduling process includes selecting the observation and download time windows and determining their start times, the problem involves the time window, data storage, energy consumption, data transmission, sensor roll, sensor pitch, attitude stabilization, turn-on time, and turn-off time.

3.1.1 Time Window

As illustrated in Figure 3, when the AEOS moves above the ground target, it can see the target for a period of time, which is called the VPVTW. In actual applications, due to the low quality of the maneuver imaging, AEOSs usually do not carry out maneuvers while imaging to satisfy the user's resolution requirements. Therefore, it is necessary to discretize a VPVTW into multiple VTWs, the number of which depends on the discrete granularity ΔP. In fact, each VTW is similar to a visible time window of the CEOS. Here, for convenience, we will abbreviate the fixed-pitch visible time windows as VTW. During a given scheduling period, more than one VTW generally exists between an AEOS and a target. Furthermore, the VTW is often longer than the observation time window (OTW) required for the observation time of the task (Hao et al. 2014). Therefore, in the AEOS scheduling, not only the VTW but also the precise start time of the observation must be selected (Xu et al. 2016). The communication antennas of AEOSs cover very wide areas and generally do not need to be maneuvered. Thus, we do not discretize the visible time windows of the ground stations. For simplicity, we label the VTWs between the satellites and task as the task VTWs and the VTWs between the satellites and ground station as the ground station VTWs.

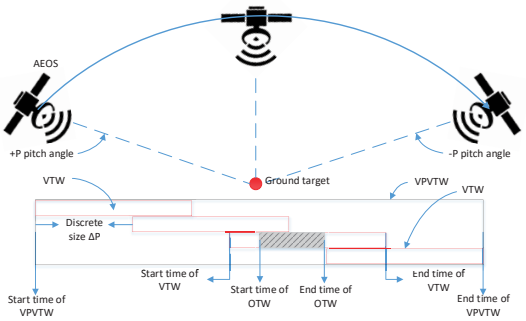

Figure 3 Time Window

3.1.2 Data Storage

The AEOS has onboard data storage that temporarily stores the task observation data (Roychowdhury et al. 2017). Once the data are transmitted to the ground station, the storage is released (Chen et al. 2016). Therefore, the real-time memory capacity is changed dynamically during the observation process.

3.1.3 Energy Consumption

Each operation, such as observation, maneuver, and downloading, consumes energy. The AEOS has limited energy, and the energy consumption cannot exceed the maximum energy capacity in each orbit circle. Therefore, the AEOS's residual energy also changes dynamically during the observation process.

3.1.4 Data Transmission

The ground station can receive the observation data transmitted by the satellite. As with the observation task, the data transmission must be completed within the ground station VTW (Song et al. 2018). Because data transmission will consume the working hours of the satellites, full use should be made of the onboard

storage to minimize the amount of data transmission (Peng et al. 2017).

3.1.5 Sensor Roll

The AEOS sensor has a field of view and a maximum roll angle. Each observation can form a wide strip on the ground at the maximum roll angle range. Clearly, it is only possible for the resource to complete the observation if the target is within the maximum roll angle range (Mao et al. 2012). If a target is not below the AEOS, the AEOS must rotate its sensor to ensure that the strip can cover the target. At the same time, the AEOS will consume time and energy when performing roll operations. Therefore, we should minimize the number of roll operations to conserve satellite energy.

3.1.6 Sensor Pitch

The AEOS sensor can pitch forward and backward, which can extend the number of VTWs to increase the opportunity for task insertion. Similarly, the pitch operation of the sensor also consumes time and satellite energy. Therefore, the number of pitch operations should be reduced as much as possible.

3.1.7 Attitude Stabilization

The AEOS will generate vibrations after a maneuver operation, and a certain amount of time is required to stabilize. Generally, the attitude stabilization time of the AEOS is fixed. After this time, the AEOS can enter a stable state and observe the ground target.

3.1.8 Turn-on and Turn-off Time

The AEOS will observe the ground target when it turns its sensor on, which consumes energy and storage. To save energy and storage, the sensor should be turned off after each observation and turned on again when the next ground target is observed.

3.2 Problem Processing

3.2.1 Problem Assumptions

In practice, the AEOS scheduling for emergency tasks is rather complicated due to the many constraints and user requirements. Therefore, some assumptions are made to simplify the problem, ignoring some non-significant constraints.

(i) When the ground station VTW between the AEOS and the ground station is scheduled, the data on the AEOS is transmitted to the ground station. The transmission time length is the ground station VTW length, and the storage is cleared after the transmission.

(ii) The start time of the VTW changes linearly with the pitch angle of the AEOS sensor. This assumption is used to calculate the impact of the pitch angle on the VTW.

(iii) A target only needs to be observed one time, and all the targets have the same observation duration.

(iv) There is no time conflict between the data downloading and the task imaging for the AEOSs, they can transmit data while imaging.

3.2.2 Scheduling Process

To address the AEOS scheduling problem for emergency tasks, a novel algorithm is proposed, which is used to deal with the arriving emergency tasks, as illustrated in Figure 4. First, the time windows are processed to divide VPVTWs and filter task VTWs before scheduling. The AEOS scheduling model is then established to maximize the ratio of the total scheduled task value to the total task value. Finally, the MISDR algorithm is designed to schedule the tasks and generate a local adjustment scheduling scheme rapidly.

4. Scheduling Model

The pitch angle changes with time in a VPVTW, which will seriously affect the image quality when observing. It is difficult to establish a scheduling model that includes the simultaneous changes of time and angle. Therefore, in this study, a time window division rule is first carried out before the scheduling model is established, which can convert a VPVTW to multiple VTWs. Then, a time window filter-

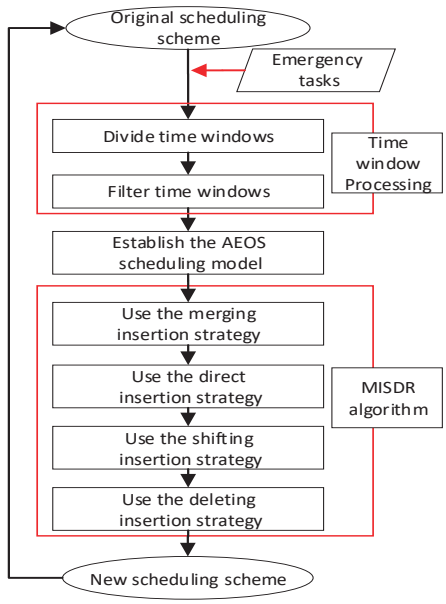

Figure 4 AEOS Scheduling Process for Emergency Tasks

ing rule is designed to eliminate the invalid visible time window and reduce the problem scheduling scale. Finally, an AEOS scheduling model with the limitations of the pitch and roll capabilities is designed for the emergency task scheduling problem.

4.1 Scheduling Symbols

The scheduling process involves satellites, ground stations, tasks, time windows and so on. In order to introduce the scheduling model conveniently, the relevant symbols and definitions are listed in Table 2.

4.2 Time Window Division

To ensure that the long time window continuity of the VPVTW is retained and the operational requirements of the subsequent VTW merging strategy are met during the division, the following principles must be followed in the time window division. (i) The overlap time of two consecutive visible time windows must be greater than the task duration time, and sufficient time must be left for the maneuver for the newly added pitch angle. (ii) All VPVTWs except the first and last have the same discrete granularity and discretize from 0° pitch angle

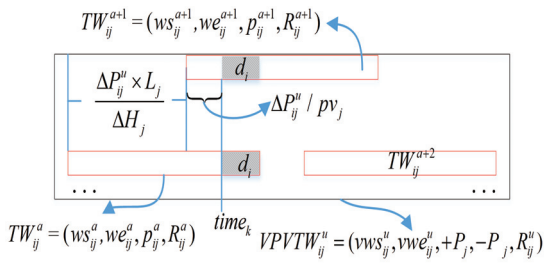

Figure 5 The Variable-Pitch Visible Time Window Division

to both sides to ensure that the following merging strategy can be implemented.

- Discrete Granularity
  As illustrated in Figure 5, based on a variable-pitch visible time window, denoted as $VPVTW_{ij}^{u} = (vws_{ij}^{u}, vwe_{ij}^{u}, +P_{ij}^{u}, -P_{ij}^{u}, R_{ij}^{u})$, between the AEOS s_j and task t_j, the long time window continuity is that the VTW TW_{ij}^{a} is available before time $time_k$ and the VTW TW_{ij}^{a+1} is available after time $time_k$. Therefore, we let $L_j = \frac{\Delta P_{ij}^{u}\times L_j}{\Delta H_j} + \frac{\Delta P_{ij}^{u}}{pv_j} + d_i$ and keep enough time for pitching maneuver, which can be converted to $\Delta P_{ij}^{u} = \frac{(L_j-d_i)\times\Delta H_j\times pv_j}{L_j\times pv_j+\Delta H_j}$. To ensure the VTW merging strategy can be carried out, we let $\Delta P = min\{\Delta P_{ij}^{u} | t_i \in T, s_j \in S, u \in \{1,\cdots,N_{VP_{ij}}\}\}$ for all VPVTWs, which can guarantee enough overlap time for the VTWs belonging to a VPVTW. Thus, the same discrete granularity ΔP can be obtained.
- Division Rule
  Based on the discrete granularity, for a VPVWTW $VPVTW_{ij}^{u} = (vws_{ij}^{u}, vwe_{ij}^{u}, +P_j, -P_j, R_{ij}^{u})$, we can calculate the VTW number $N_F = 2\times\lceil\frac{P_j}{\Delta P}\rceil+1$. We can then calculate a visible time window $TW_{ij}^{a} = (ws_{ij}^{a}, we_{ij}^{a}, R_{ij}^{a}, p_{ij}^{a})$, where

$$\begin{cases} ws_{ij}^{a} = vws_{ij}^{u} \\ we_{ij}^{a} = vws_{ij}^{u} + L_j, \\ p_{ij}^{a} = P_j \\ R_{ij}^{a} = R_{ij}^{u} \end{cases}$$

Table 2 The Table of Symbols

Sysmbol	Definition
$S = \{s_1, \cdots, s_j, \cdots, s_{N_S}\}$	S is the AEOS set, N_S is its AEOS number.
$G = \{g_1, \cdots, g_k, \cdots, g_{N_G}\}$	G is the ground station set, N_G is its ground station number.
$T = \{DET \bigcup DGT \bigcup ET \bigcup GT\}$	Task set.
$DET = \{t_1, \cdots, t_{N_{DET}}\}$	DET is the scheduled emergency task set, N_{DET} is its task number.
$DGT = \{t_{N_{DET}+1}, \cdots, t_{N_{DET}+N_{DGT}}\}$	DGT is the scheduled general task set, N_{DGT} is its task number.
$ET = \{t_{N_{DET}+N_{DGT}+1}, \cdots, t_{N_{DET}+N_{DGT}+N_{ET}}\}$	ET is the unscheduled emergency task set, N_{ET} is its task number.
$GT = \{t_{N_{DET}+N_{DGT}+N_{ET}+1}, \cdots, t_{N_{DET}+N_{DGT}+N_{ET}+N_{GT}}\}$	GT is the unscheduled general task set, N_{GT} is its task number.
$N_T = \{N_{DGT} + N_{DET} + N_{ET} + N_{GT}\}$	Total task number.
$t_i = (tv_i, d_i, dl_i)$	t_i is the i-th task in T, tv_i, d_i and dl_i are its task value, task duration time, and task completion deadline, respectively.
$TW_i = \{TW_{i1}, \cdots, TW_{ij}, \cdots, TW_{iN_S}\}$	VTW set of t_i.
$TW_{ij} = \{TW_{ij}^1, \cdots, TW_{ij}^a, \cdots, TW_{ij}^{N_{TW_{ij}}}\}$	TW_{ij} is the VTW set between t_i and s_j, $N_{TW_{ij}}$ is its VTW Number.
$TW_{ij}^a = (ws_{ij}^a, we_{ij}^a, p_{ij}^a, R_{ij}^a)$	TW_{ij}^a is the a-th VTW between t_i and s_j, ws_{ij}^a, we_{ij}^a, p_{ij}^a and R_{ij}^a are its start time, end time, pitch angle and ideal roll angle.
$GW_k = \{GW_{k1}, \cdots, GW_{kj}, \cdots, GW_{kN_S}\}$	VTW set of g_k.
$GW_{kj} = \{GW_{kj}^1, \cdots, GW_{kj}^b, \cdots, GW_{kj}^{N_{GW_{kj}}}\}$	GW_{kj} is the VTW set between g_k and s_j, $N_{GW_{kj}}$ is its VTW Number.
$GW_{kj}^b = (ws_{kj}^b, we_{kj}^b)$	GW_{kj}^b is the b-th VTW between g_k and s_j, ws_{kj}^b and we_{kj}^b are its start and end times.
ΔH_j	Horizontal field of view in pitch direction of s_j.
ΔV_j	Vertical field of view in roll direction of s_j.
pv_j	Pitch velocity of s_j.
rv_j	Roll velocity of s_j.
b_j	Turn-on time of s_j.
e_j	Turn-off time of s_j.
as_j	Attitude stabilization time of s_j.
L_j	Time from the ground target is covered until not covered by the observation band of s_j with a fixed pitch angle.
M_j	Maximum storage capacity of s_j.
E_j	Maximum energy capacity within each orbit circle of s_j.
N_{C_j}	Maximum orbit circle number of s_j.
α_j	Storage capacity required per unit time observation of s_j.
β_j	Energy capacity required per unit time observation of s_j.
ρ_j	Energy capacity required per unit time data transition of s_j.
ω_j	Energy capacity required per unit time maneuver of s_j.
Δt_j	Maximum power-on duration of s_j.
$VPVTW_{ij}^u = (vws_{ij}^u, vwe_{ij}^u, +P_j, -P_j, R_{ij}^u)$	$VPVTW_{ij}^u$ is the u-th VPVTW between t_i and s_j, vws_{ij}^u,vwe_{ij}^u,$+P_j$,$-P_j$ and R_{ij}^u are its earliest visible time, latest visible time, maximum pitch angle and ideal pitch angle.
$u \in \{1, \cdots, N_{VP_{ij}}\}$	u and $N_{VP_{ij}}$ are the index and number of VPVTW between t_i and s_j.
ΔP_{ij}^u	Sub-discrete granularity.
ΔP	Discrete granularity.
te_{kj}^b	Observation end time of the k-th VTW between g_k and s_j.
ts_{ij}^a	Observation start time of the a-th VTW between t_i and s_j.
te_{ij}^a	Observation end time of the a-th VTW between t_i and s_j.
r_{ij}^a	Observation roll angle of the a-th VTW between t_i and s_j.
TWT_{ij}^a	Tasks whose observation time windows overlap with TW_{ij}^a.
H	Scheduling horizon.
H_s	Start time of the scheduling horizon.
$MT = \{MT_1, \cdots, MT_u, cdots, MT_{N_{MT}}\}$	MT is the set of merging time window set, N_{MT} is the number of times that multiple time windows are executed at a time.
$MT_u = \{TW_{ij}^a, \cdots, TW_{i'j'}^{a'}\}$	The u-th is merging time window set executed at a time.

if $a = 1$;

$$\begin{cases} ws_{ij}^a = \frac{vws_{ij}^u + vwe_{ij}^u}{2} - \frac{(\frac{N_F+1}{2} - a) \times \Delta P + \Delta H_j}{\Delta H_j} \times \frac{L_j}{2} \\ we_{ij}^a = \frac{vws_{ij}^u + vwe_{ij}^u}{2} - \frac{(\frac{N_F+1}{2} - a) \times \Delta P - \Delta H_j}{\Delta H_j} \times \frac{L_j}{2}, \\ p_{ij}^a = (\frac{N_F+1}{2} - a) \times \Delta P \\ R_{ij}^a = R_{ij}^u \end{cases}$$

if $1 < a < N_F$; or

$$\begin{cases} ws_{ij}^a = vwe_{ij}^u - L_j \\ we_{ij}^a = vwe_{ij}^u, \\ p_{ij}^a = -P_j \\ R_{ij}^a = R_{ij}^u \end{cases}$$

if $a = N_F$. As illustrated in Figure 5, suppose $N_F = 3$, we can get $TW_{ij}^1 = (vws_{ij}^u, vws_{ij}^u + L_j, P_j, R_{ij}^u)$, $TW_{ij}^2 = (\frac{vws_{ij}^u + vwe_{ij}^u - L_j}{2}, \frac{vws_{ij}^u + vwe_{ij}^u + L_j}{2}, 0, R_{ij}^u)$ and $TW_{ij}^3 = (vwe_{ij}^u - L_j, vwe_{ij}^u, -P_j, R_{ij}^u)$. p_{ij}^a is positive in the forward direction; otherwise, it is non-positive. Through division, multiple VPVTWs can be converted into more VTWs.

4.3 Time Window Filtering

The task VTWs in the scheduling horizon and before the completion deadline are filtered to reduce the complexity of the problem. As shown in Figure 6, the scheduling horizon is H and the start time of H is H_s, only the VTWs after H_s and before dl_i are retained. Through this process, some invalid VTWs are deleted, and some valid VTWs, including TW_{ij}^1, TW_{ij}^2, TW_{ij}^3, TW_{ij}^4, TW_{ij}^5, TW_{ij}^6, $TW_{i(j+1)}^1$, $TW_{i(j+1)}^2$ and $TW_{i(j+1)}^3$, are gained for task t_i. Therefore, the scale of the scheduling problem can be reduced so that the scheduling efficiency can be improved significantly.

4.4 Scheduling Objective and Constraints

According to the scheduling problem, we establish an objective function to maximize the value of scheduled tasks and corresponding constraints that include task observation number, task deadline, time window conflict, observation time, observation angle, satellite storage, satellite energy and observation merging.

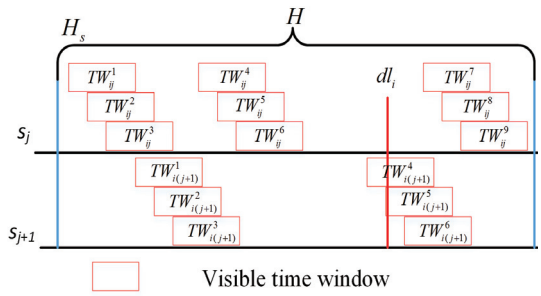

Figure 6 Time Window Filtering Diagram

In order to better understand the value completion of scheduled tasks, the objective function is designed as the ratio of the total scheduled task value to the total task value, which can guarantee the result between 0 and 1.

$$\max \left\{ [\sum_{i=1}^{N_T} \sum_{j=1}^{N_S} \sum_{a=1}^{N_{TW_{ij}}} (x_{ij}^a \times tv_i)] / \sum_{i=1}^{N_T} tv_i \right\} \quad (1)$$

where x_{ij}^a is a decision variable defined as follows:

$$x_{ij}^a = \begin{cases} 1, & t_i \text{ is observed in } TW_{ij}^a \\ 0, & \text{otherwise} \end{cases} \quad (2)$$

(i) Each task can only be observed at most once, and the transmission time must be before the task deadline. These constraints are expressed as follows:

$$C_1 : \begin{cases} \sum_{j=1}^{N_S} \sum_{a=1}^{N_{TW_{ij}}} x_{ij}^a \le 1, & \forall t_i \in T \\ (dl_i - te_{kj}^b) \times x_{ij}^a \ge 0, & \forall TW_{ij}^a \in W_{kj}^b \end{cases} \quad (3)$$

In this study, we assume that the transmission duration is equal to the ground station VTW duration. Thus, te_{kj}^b is equal to we_{kj}^b. Moreover, as illustrated in Figure 7, a ground station VTW is virtualized on each satellite at the scheduling time, and the VTWs that are scheduled between two consecutive ground station VTWs are denoted as W_{kj}^b.

(ii) When two tasks are performed on the same AEOS, the interval between their observation time windows must satisfy the maneu-

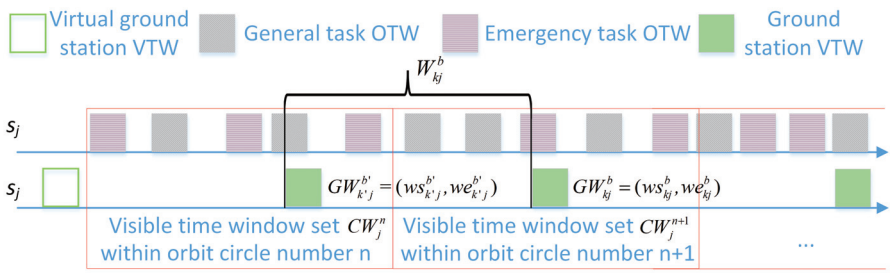

Figure 7 W_{kj}^{b} and CW_j^n Diagram

ver time requirements. Each AEOS cannot transmit data to two ground stations at the same time. Each ground station can only receive data from one AEOS at a time. These constraints are expressed as follows:

$$C_2:\begin{cases} x_{ij}^a+x_{i'j}^{a'}\le 1, & \begin{array}{l}\forall(TW_{ij}^a,TW_{i'j}^{a'})\in\{(TW_{ij},TW_{i'j})\backslash \\ \{(TW_{ij}^a,TW_{i'j}^{a'})|TW_{ij}^a,TW_{i'j}^{a'}\in MT_u, \\ u\in\{1,\cdots,N_{MT}\}\},t_i,t_{i'}\in T,s_j\in S,\end{array} \\ y_{kj}^b+y_{k'j}^{b'}\le 1, & \begin{array}{l}[ts_{ij}^a-as_j-\frac{|r_{ij}^a-r_{i'j}^{a'}|}{rv_j}-\frac{|p_{ij}^a-p_{i'j}^{a'}|}{pv_j}-b_j,te_{ij}^a+e_j]\cap \\ [ts_{i'j}^{a'}-as_j-\frac{|r_{ij}^a-r_{i'j}^{a'}|}{rv_j}-\frac{|p_{ij}^a-p_{i'j}^{a'}|}{pv_j}-b_j,te_{i'j}^{a'}+e_j]\ne\emptyset \\ \forall s_j\in S,g_k,g_{k'}\in G,b\in\{1,\cdots,N_{GW_{kj}}\}, \\ b'\in\{1,\cdots,N_{GW_{k'j}}\},[ws_{kj}^b,we_{kj}^b]\cap[ws_{k'j}^{b'},we_{k'j}^{b'}]\ne\emptyset\end{array} \\ y_{kj}^b+y_{kj'}^{b'}\le 1, & \begin{array}{l}\forall s_j,s_{j'}\in S,g_k\in G,b\in\{1,\cdots,N_{GW_{kj}}\}, \\ b'\in\{1,\cdots,N_{GW_{kj'}}\},[ws_{kj}^b,we_{kj}^b]\cap[ws_{kj'}^{b'},we_{kj'}^{b'}]\ne\emptyset\end{array}\end{cases} \tag{4}$$

where y_{kj}^b is a decision variable defined as follows:

$$y_{kj}^b=\begin{cases}1, & g_k \text{ receives image data in } GW_{kj}^b \\ 0, & \text{otherwise}\end{cases} \tag{5}$$

(iii) The observation time window of each task must be within the corresponding VTW. The observation strip must cover the ground target. These constraints are expressed as follows:

$$C_3:\begin{cases} x_{ij}^a\times(ts_{ij}^a-ws_{ij}^a)\ge 0, \\ x_{ij}^a\times(we_{ij}^a-ts_{ij}^a-d_i)\ge 0, \\ x_{ij}^a\times|r_{ij}^a-R_{ij}^a|\le\frac{\Delta V_j}{2}, \end{cases} \quad \begin{array}{l}\forall t_i\in T,s_j\in S, \\ a\in\{1,\cdots,N_{TW_{ij}}\}\end{array} \tag{6}$$

(iv) The storage of each AEOS during the observations cannot exceed the maximum storage capacity, and the energy consumed within each orbit circle cannot exceed the maximum energy capacity. These constraints are expressed as follows:

$$C_4:\begin{cases} y_{kj}^b\times(\sum\limits_{\forall TW_{ij}^a\in\{W_{kj}^b\backslash MT\}}x_{ij}^a\times d_i+ \\ \sum\limits_{u=1}^{N_{MT}}(\max\limits_{\forall TW_{ij}^a\in\{W_{kj}^b\cap MT_u\}}\{te_{ij}^a\}- \\ \min\limits_{\forall TW_{ij}^a\in\{W_{kj}^b\cap MT_u\}}\{ts_{ij}^a\}))\times\alpha_j\le M_j, \\ (\sum\limits_{\forall TW_{ij}^a\in\{CW_j^n\backslash MT\}}x_{ij}^a\times d_i+ \\ \sum\limits_{u=1}^{N_{MT}}(\max\limits_{\forall TW_{ij}^a\in\{CW_j^n\cap MT_n\}}\{te_{ij}^a\}- \\ \min\limits_{\forall TW_{ij}^a\in\{CW_j^n\cap MT_n\}}\{ts_{ij}^a\}))\times\beta_j+ \\ \sum\limits_{\forall GW_{kj}^b\in CW_j^n}y_{kj}^b\times d_k\times\rho_j+ \\ \sum\limits_{TW_{ij}^a\in CW_j^n}\sum\limits_{\substack{\forall TW_{ij}^{a'}\in CW_j^n \\ ,TW_{ij}^{a'}\ne TW_{ij}^a}}l(x_{ij}^a,x_{i'j}^{a'})\times \\ (\frac{|r_{ij}^a-r_{i'j}^{a'}|}{rv_j}+\frac{p_{ij}^a-p_{i'j}^{a'}}{pv_j})\times\omega_j\le E_j, \end{cases} \quad \begin{array}{l}\forall s_j\in S,g_k\in G, \\ b\in\{1,\cdots,N_{GW_{kj}}\} \\ \\ \\ \\ \\ \\ \forall s_j\in S, \\ n\in\{1,\cdots,N_{C_j}\}\end{array} \tag{7}$$

where $l(x_{ij}^a,x_{i'j}^{a'})$ is a is used to judge whether two observation time windows are adjacent. If they are adjacent, it is 1; otherwise, it is 0. As shown in Figure 7, CW_j^n indicates the set of ground station VTWs and OTWs that are scheduled within the n-th orbit of s_j.

(v) Not every task can be merged with other tasks, which is limited by angle and time constraints. (a) Angle constraint: The distance of ideal roll angles of any two OTWs must be smaller than the vertical field of view in the roll direction of the AEOS, and their pitch angles must be equal. (b) Time constraint: The merging observation duration of any two OTWs must be within a certain time range. These constraints are expressed as follows:

$$C_5:\begin{cases} |R_{ij}^a-R_{i'j}^{a'}|\le\Delta V_j, & \begin{array}{l}\forall TW_{ij}^a,TW_{i'j}^{a'}\in MT_u, \\ u\in\{1,\cdots,N_{MT}\}\end{array} \\ p_{ij}^a=p_{i'j}^{a'}, & \begin{array}{l}\forall TW_{ij}^a,TW_{i'j}^{a'}\in MT_u, \\ u\in\{1,\cdots,N_{MT}\}\end{array} \\ \max\limits_{TW_{ij}^a\in MT_u}\{te_{ij}^a\}-\min\limits_{TW_{ij}^a\in MT_u}\{ts_{ij}^a\}\le\Delta t_j, & \forall u\in\{1,\cdots,N_{MT}\} \\ r_{ij}^a=\frac{\max\limits_{TW_{i'j}^{a'}\in MT_u}\{R_{i'j}^{a'}\}+\min\limits_{TW_{i'j}^{a'}\in MT_u}\{R_{i'j}^{a'}\}}{2}, & \begin{array}{l}\forall TW_{ij}^a\in MT_u, \\ u\in\{1,\cdots,N_{MT}\}\end{array}\end{cases} \tag{8}$$

5. Scheduling Algorithm

The CEOS scheduling problem is an NP-complete problem (Hall et al. 1994). The AEOS scheduling problem for emergency tasks is similar to it. Similarly, efficient solutions to the problem with numerous resources and tasks cannot be provided in a limited time. In particular, AEOSs can provide more observation opportunities than CEOSs, which will lead to a more complex scheduling problem. Therefore, it is difficult to solve with exact algorithms. In addition, since emergency tasks are highly urgent and have relatively short deadlines, AEOS scheduling for such tasks is usually required to be completed in tens of seconds, or even seconds. Thus, the meta-heuristic algorithms are not suitable for the AEOS scheduling for emergency tasks. Finally, we decide to design a heuristic algorithm to solve the problem.

Based on the above scheduling model, to quickly respond to the needs of emergency tasks and complete as much task value as possible with limited AEOSs, an effective algorithm based on merging insertion, direct insertion, shifting insertion, deleting insertion, and reinsertion strategies (MISDR) is proposed to deal with the AEOS scheduling problem for emergency tasks. In particular, different from the previous papers, based on the pitch and roll capabilities of the AEOS, a merging insertion strategy is designed to include similar tasks in the same observation strip, which can increase the flexibility of the task time window selection and save the AEOS resources. Based on the fact that a VTW is longer than the task observation time, the task shifting strategy is designed. Under satisfying the observation constraints, the conflicting tasks can be moved forward or backward within their own VTWs, which can improve the insertion possibility of emergency tasks. Simultaneously, the flexible insertion of the ground station VTWs is considered to reduce the impact of the storage capacity limitation. To further improve algorithm efficiency, two heuristic factors, the urgency degree of an emergency task and the merging degree of a time window, are designed to guide the task insertion sequence and task merging time window selection.

5.1 Heuristic Factors

An urgency degree and a merging degree are designed to sort the unscheduled emergency task set and select the merging position of the emergency task, respectively.

(i) The urgency degree of an emergency task t_i is denoted by $\delta_i = \frac{tv_i \times \max\limits_{t_{i'} \in ET \cup DET} \{N_{TW_{i'}} - N_{TW_i}\}}{\max\limits_{t_{i'} \in ET \cup DET} \{N_{TW_{i'}} \times tv_{i'}\}} / \frac{dl_i - H_s}{\max\limits_{t_{i'} \in ET \cup DET} \{dl_{i'} - H_s\}}$. Emergency tasks can be sorted from high to low based on δ_i, which arranges emergency tasks that are close to the deadline and have a high value and less number of time windows to be completed as early as possible. (ii) The merging degree of a VTW TW_{ij}^a is represented by $\psi_{ij}^a = \max\{\frac{\min\{we_{ij}^a, te_{i'j}^{a'}\} - \max\{ws_{ij}^a, ts_{i'j}^{a'}\}}{d_i} \times \frac{dl_i - ws_{ij}^a}{dl_i - H_s}, TW_{i'j}^{a'} \in TWT_{ij}^a\}$. When a task t_i has multiple merging opportunities, the time window with a larger value of ψ_{ij}^a is selected, which can provide guidance to choose a time window with a higher overlap of time windows and an earlier task completion time for the scheduling.

5.2 MISDR Algorithm

To present the algorithm clearly, the conflicting tasks and conflict conception are firstly introduced. Conflicting tasks, which cause the task t_i not to be inserted into the scheduling scheme directly, can be divided into three categories. (i) Tasks whose observation time windows overlap with TW_{ij}^a, which is denoted as TWT_{ij}^a. To traverse the idle time period between conflict tasks better, the previous time window and the next time window of the TW_{ij}^a are placed into TWT_{ij}^a. (ii) Tasks whose observation time windows have the same previous and next ground station VTWs as TW_{ij}^a. If task t_i is executed within TW_{ij}^a, the AEOS will be

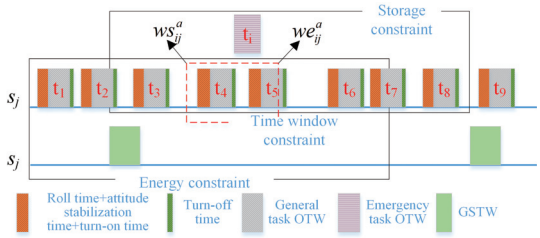

Figure 8 Conflict Task and Conflict Diagram

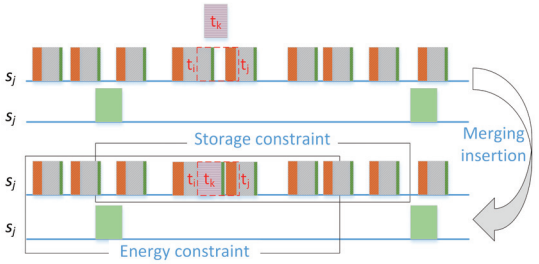

Figure 9 Merging Insertion Strategy

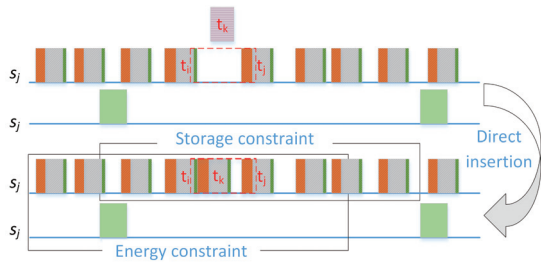

Figure 10 Direct Insertion Strategy

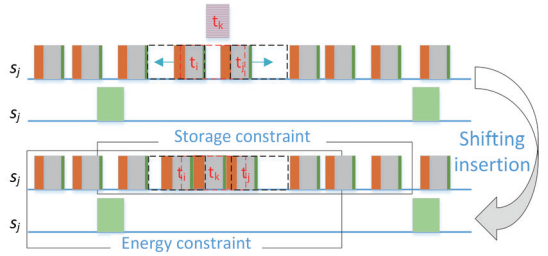

Figure 11 Shifting Insertion Strategy

overloaded. These tasks are denoted as ST_{ij}^a. (iii) Tasks whose observation time windows and TW_{ij}^a are in the same orbit circle. If task t_i is executed within TW_{ij}^a, the AEOS energy is insufficient. These tasks are denoted as ENT_{ij}^a.

A conflict is a combination of conflicting tasks, consisting of at least one task. The conflicts can be divided into three categories. (i) When the conflict is deleted, the observation duration of the task t_i can be satisfied. These conflicts are denoted as TWC_{ij}^a. (ii) When the conflict is deleted, the observation duration of the task t_i can be satisfied and the overload of the AEOS cannot occur. These conflicts are denoted as SC_{ij}^a. (iii) When the conflict is deleted, the observation duration of the task t_i can be satisfied and the AEOS energy shortage cannot occur. These conflicts are denoted as ENC_{ij}^a.

As shown in Figure 8, when the task t_i is inserted within the VTW $TW_{ij}^a = [ws_{ij}^a, we_{ij}^a]$, if constraints C_3 and C_4 are not satisfied, TWT_{ij}^a, TWC_{ij}^a, ST_{ij}^a, SC_{ij}^a, ENT_{ij}^a and ENC_{ij}^a are $\{\{t_3\}\{t_4\}\{t_5\}\{t_6\}\}$, $\{\{t_4\}\{t_5\}\}$, $\{\{t_2\}\{t_3\}\{t_4\}\{t_5\}\{t_6\}\{t_7\}\{t_8\}\}$, $\{\{t_3\}\{t_4\}\{t_5\}\{t_6\}\{t_7\}\{t_8\}\}$, $\{\{t_1\}\{t_2\}\{t_3\}\{t_4\}\{t_5\}\{t_6\}\{t_7\}\}$ and $\{\{t_1\}\{t_2\}\{t_3\}\{t_4\}\{t_5\}\{t_6\}\}$, respectively.

The MISDR algorithm includes merging insertion, direct insertion, shifting insertion, deleting insertion, and reinsertion strategies. Simultaneously, if the storage constraints are not satisfied during executing these strategies, the ground station VTW insertion is considered.

(i) Merging insertion strategy

As illustrated in Figure 9, in the scheduling scheme, if $TWT \neq \emptyset$, where $TWT = \sum_{j=1}^{N_S} \sum_{a=1}^{N_{TW_{ij}}} TWT_{ij}^a$, the VTWs of the waiting task t_i can be sorted from high to low based on ψ_{ij}^a. The sorted VTWs are traversed to select the one that satisfies constraints C_3, C_4 and C_5 to merge with the conflicting task.

(ii) Direct insertion strategy

As illustrated in Figure 10, if the waiting task t_i can be inserted into an idle time of the scheme while satisfying constraints C_3 and C_4, it is directly inserted into the scheme.

(iii) Shifting insertion strategy

As illustrated in Figure 11, when the waiting task t_i cannot be scheduled by the above strategies, the tasks before it are moved forward and the tasks after it are moved backward in their own VTWs while satisfying constraints C_3 and C_4, after which the idle time within a VTW of the waiting task t_i is calculated. If

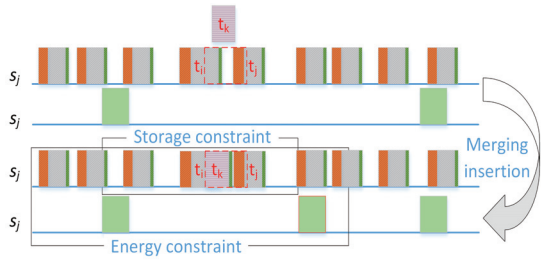

Figure 12 Merging Insertion Strategy Based on Ground Station VTW Insertion

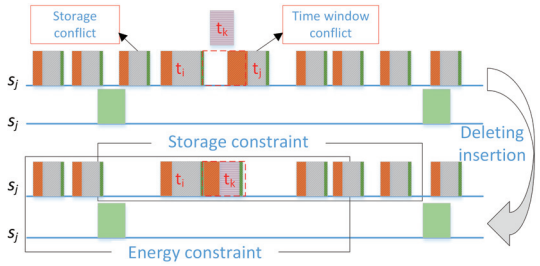

Figure 13 Deleting Insertion Process

the waiting task t_i can be inserted into the idle time while satisfying constraints C_3 and C_4, the shifting strategy is performed and the waiting task t_i is inserted.

(iv) Merging insertion strategy based on ground station VTW insertion

As illustrated in Figure 12, if the VTW of the waiting task t_i cannot be scheduled by the merging insertion strategy only due to AEOS overload, a suitable ground station VTW can be inserted into the scheme with satisfying constraint C_4 and C_5, then the merging insertion strategy is executed for the waiting task t_i.

(v) Direct insertion strategy based on ground station VTW insertion

Similar to (iv), if the VTW of the waiting task t_i cannot be scheduled by the direct insertion strategy only due to AEOS overload, a suitable ground station VTW can be inserted into the scheme with satisfying constraint C_4, then the direct insertion strategy is executed for the waiting task t_i.

(vi) Shifting insertion strategy based on ground station VTW insertion

Similar to (iv), if the VTW of the waiting task t_i cannot be scheduled by the shifting strategy only due to AEOS overload, a suitable ground station VTW can be inserted into the scheme with satisfying constraint C_4, then the shifting insertion strategy is executed for the waiting task t_i.

(vii) Deleting insertion strategy

As illustrated in Figure 13, for each VTW TW_{ij}^a of the waiting task t_i, the time window conflict with a minimum sum value in TWC_{ij}^a is selected as $NTWC_{ij}^a$. SC is recalculated based on the assumption that all tasks in $NTWC_{ij}^a$ are deleted, and the storage conflict with a minimum sum value in SC_{ij}^a is selected as NSC_{ij}^a. We then recalculate ENC_{ij}^a based on the assumption that all tasks in $NTWC_{ij}^a \bigcup NSC_{ij}^a$ are deleted, and the energy conflict with a minimum sum value in ENC_{ij}^a is selected as $NENC_{ij}^a$. Finally, the $NTWC_{ij}^a \bigcup NSC_{ij}^a \bigcup NENC_{ij}^a$ is added to the deleting conflict set NC_i. After the VTWs of the waiting task t_i have been traversed, if the NC_i^k with a minimum sum value in NC_i has a smaller value than the waiting task t_i, NC_i^k is deleted and the waiting task is inserted in the scheme.

(viii) Reinsertion strategy

All the tasks deleted by the deletion strategy are added to the corresponding unscheduled task set and are reinserted during the process of traversing the task set.

Based on the above strategies, the scheduling algorithm flow is shown in Algorithm 1.

The time complexity of the MISDR algorithm can be estimated according to the algorithm strategies and flow. We assume that $\bar{N}_{TW}$ is the maximum of single task VTW number and single ground station VTW number. The time complexity of line 1 is $O(N_{ET} + N_{DET} + N_{ET}^2)$. For lines 2, 3 and 4, the time complexity is $O((N_{ET} + N_{DET}) \times \bar{N}_{TW} \times N_T)$. The time complexity of lines 2 and 6 is $O((N_{ET} + N_{DET}) \times \bar{N}_{TW}^2)$. For lines 2 and 7-12, the time complexity is $O((N_{ET} + N_{DET}) \times \bar{N}_{TW} \times N_T)$. The time complexity of lines 2 and 13-21 is

Algorithm 1 MISDR Algorithm

Input: The unscheduled emergency tasks, the unscheduled general task set, the scheduled emergency tasks, the scheduled general task set, the original scheduling scheme

Output: The new scheduling scheme

1: Calculate δ_i for $t_i \in ET$ and sort ET by it from high to low
2: **for** t_i in ET **do**
3: **for** $TW_{ij}^a = (ws_{ij}^a, we_{ij}^a, p_{ij}^a, R_{ij}^a)$ in TW_i of t_i **do**
4: Calculate merging degree ψ_{ij}^a for visible time window TW_{ij}^a
5: **end for**
6: Sort TW_i of t_i by ψ_{ij}^a from high to low
7: **if** t_i is inserted by strategy (i) **then**
8: Insert t_i by merging with other tasks and remove t_i from ET
9: **else if** t_i is inserted by strategy (ii) **then**
10: Insert t_i and remove t_i from ET
11: **else if** t_i is inserted by strategy (iii) **then**
12: Insert t_i by shifting conflict tasks and remove t_i from ET
13: **else if** t_i is inserted by strategy (iv) **then**
14: Insert a suitable ground station visible time window
15: Insert t_i by merging with other tasks and remove t_i from ET
16: **else if** t_i is inserted by strategy (v) **then**
17: Insert a suitable ground station visible time window
18: Insert t_i and remove t_i from ET
19: **else if** t_i is inserted by strategy (vi) **then**
20: Insert a suitable ground station visible time window
21: Insert t_i by shifting conflict tasks and remove t_i from ET
22: **else if** t_i is inserted by strategy (vii) **then**
23: Insert t_i by deleting conflict tasks and remove t_i from ET, subsequently add conflict tasks to GT and ET
24: **end if**
25: **end for**
26: Insert $t_i \in GT$ by strategy (i)(ii)(iii)(iv)(v)(vi) and (vii) without heuristic factors

$O((N_{ET} + N_{DET}) \times \bar{N}_{TW} \times N_T \times N_G \times \bar{N}_{TW})$. For lines 2, 22 and 23, the time complexity is $O((N_{ET} + N_{DET}) \times \bar{N}_{TW} \times N_T)$. Thus, the time complexity is $O((N_{ET}+N_{DET})\times N_T \times N_G \times \bar{N}_{TW}^2)$ for lines 1 to 25. Because the scheduling flow of general tasks is similar to that of emergency tasks, the time complexity of line 26 is $O((N_{GT} + N_{DGT}) \times N_T \times N_G \times \bar{N}_{TW}^2)$. As a result, the total time complexity is calculated as follows: $O((N_{ET} + N_{DET} + N_{GT} + N_{DGT}) \times N_T \times N_G \times \bar{N}_{TW}^2) = O({N_T}^2 \times N_G \times \bar{N}_{TW}^2)$.

6. Experimental Simulation and Discussion

To verify the scheduling algorithm, we carried out multiple experiments by comparing the results of the proposed algorithm with those of the ISDR and TMBSR-DES algorithms, and analyzed and summarized the experimental results.

6.1 Experimental Design

We simulated nine satellites, as indicated in Table 3. Moreover, we set the turn-on time, turn-off time, attitude stabilization time, maximum pitch angle, maximum roll angle, roll velocity, and pitch velocity equal to 7 s, 7 s, 4 s, 30°, 30°,

Table 3 Simulated Satellites

Sat_id	Sat_name	Apogee (km)	Perigee (km)	Inclination (deg)
0	AEOS 1	653	628	98.0
1	AEOS 2	633	622	98.0
2	AEOS 3	666	617	98.0
3	AEOS 4	629	626	97.9
4	AEOS 5	667	613	98.4
5	AEOS 6	491	488	97.3
6	AEOS 7	514	511	97.5
7	AEOS 8	479	471	97.4
8	AEOS 9	1206	1196	100.7

5°/s, and 5°/s, respectively. We set the maximum storage capacity, maximum energy capacity, storage capacity required per unit time observation, energy capacity required per unit time observation, energy capacity required per unit time data transition, and energy capacity per unit time maneuver equal to 200 units, 300 units, 5 units/s, 5 units/s, 5 units/s, and 5 units/s.

We simulated four ground stations on the earth surface, as indicated in Table 4, and then randomly generated 300, 400, 500, and 600 general task sets as well as 10, 20, 30, 40, 50, and 60 emergency task sets. Without loss of generality, the general task values were randomly distributed in the range 1-50, the emergency task values were randomly distributed in the range 80-100, and the durations of the task observations were randomly distributed in the range of 10-20 s.

H was defined as a 24-h scheduling horizon from July 24, 2019, 00:00:00 to July 25, 2019, 00:00:00. Prior to scheduling, we calculated the time windows for tasks and ground stations and carried out initial scheduling to generate four initial schemes for different scales of the general tasks by means of the genetic algorithm.

6.2 Algorithm Analysis

To analyze the proposed algorithm effectively, based on the four initial schemes, four groups of scheduling experiments with different emergency task scales were carried out with MISDR, TMBSR-DES, and ISDR algorithms, as indicated in Table 5.

As illustrated in Figure 14, although the running time of the proposed algorithm was worse than that of the ISDR and TMBSR-DES algorithms in some experiments, it was only 1.70% higher than that of the ISDR algorithm and 2.29% higher than that of TMBSR-DES algorithm on average. In addition, the maximum running time of the proposed algorithm was less than 643 ms. Thus, we could draw some conclusions that the running times of the algorithms are similar and the proposed algorithm could meet users' time requests. Due to the addition of a merging insertion strategy in the proposed algorithm, the merging process could take some time, but it could provide more insertion opportunities with less storage and energy and reduce the execution number of subsequent insertion strategies. Therefore, the proposed algorithm appeared the phenomena that it took more time in some experiments while less time in other experiments. Moreover, the running time of each algorithm generally increased with the number of tasks, which indicated that the growth in the task scale increased the conflict degree between tasks. Consequently, more calculation time was required to eliminate conflicts.

Figure 15 illustrated that the objective function values of the three algorithms generally decreased as the number of tasks increased, which indicated that the conflicts between

Table 4 Simulated Ground Stations

Gro_id	Gro_name	Gro_lon(deg)	Gro_lat(deg)	Gro_alt(deg)
0	BEIJING	116.595	39.04	0
1	CHANGSHA	113.037	28.25	0
2	TAIYUAN	112.585	37.82	0
3	WULUMUQI	87.395	43.86	0

Table 5 Simulated Experiments

Initial schemes		Algorithms	Scenarios	Emergency task scale
Satellite scale	General task scale			
9	300	MISDR	S1	10, 20, 30, 40, 50, 60
	400		S2	
	500		S3	
	600		S4	
	300	ISDR	S5	
	400		S6	
	500		S7	
	600		S8	
	300	TMBSR-DES	S9	
	400		S10	
	500		S11	
	600		S12	

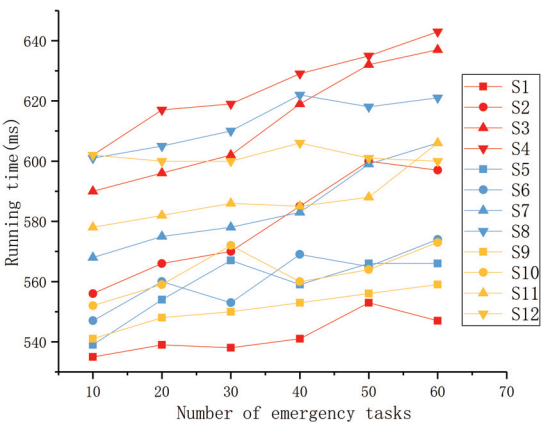

Figure 14 Algorithm Running Time

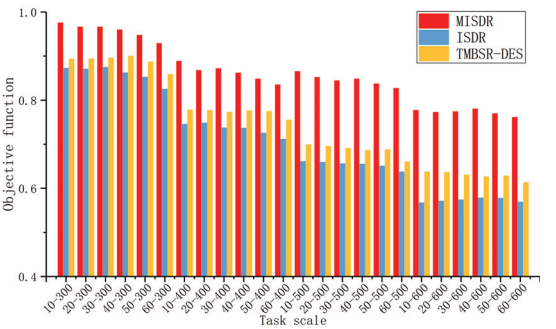

Figure 15 Objective Function

tasks dramatically increased and the opportunities for task insertion decreased when the task scale became large. Furthermore, the proposed algorithm was demonstrated to be superior to the ISDR and TMBSR-DES algorithms in the 24 groups of task scales. As shown in Figures 14, 15 and 16, the objective function of the proposed algorithm was 23.27% higher than that of the ISDR algorithm and 16.37% higher than that of TMBSR-DES algorithm on average for similar running time and observation time. This was because the tasks in the scheme and the waiting tasks could be merged to reduce task conflicts and save energy and storage capacities with the proposed algorithm, which increased the opportunities for the insertion of other waiting tasks. Furthermore, the conflicting tasks could be moved forward and backward using the proposed algorithm, which could increase the idle time for the waiting tasks. However, ISDR algorithm does not have a merging insertion strategy, and TMBSR-DES algorithm only merges waiting tasks. Thus,

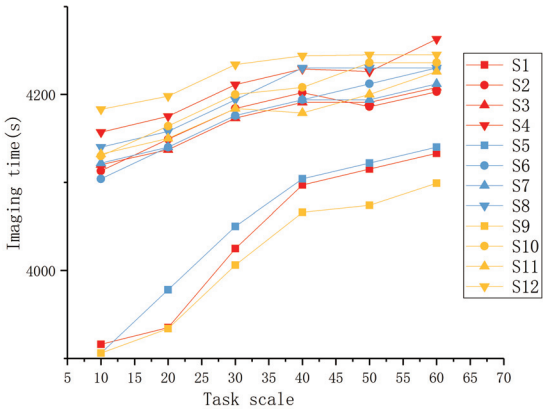

Figure 16 Observation Time

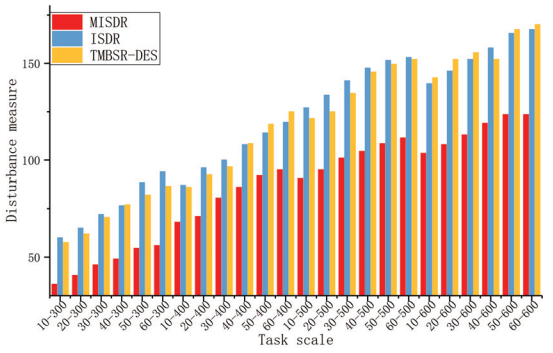

Figure 17 Disturbance Measure

these algorithms have lower flexibilities and limited conflict resolution capabilities.

Figure 17 illustrated that the disturbance measure with the proposed algorithm was significantly less than those with the ISDR and TMBSR-DES algorithms, with values 28.35% and 27.31% smaller, respectively, which indicated that the proposed algorithm exhibited a stronger conflict resolution capacity to reduce the number of tasks moved and deleted from the scheme. The disturbance measure values of the changes, which included the observation start time, end time, roll angle, and pitch angle on the single satellite, were 0.5. If these changes occurred at the same time, the disturbance measure was counted only once. The disturbance measures of the changes between AEOSs and the deletion were 1 and 1.5, respectively. These results demonstrated that the MISDR algorithm had the ability to search for the solution with a smaller disturbance measure.

6.3 Algorithm Scalability Analysis

The resources in the actual applications are not all AEOSs, there are also some CEOSs. To verify the effect of the proposed algorithm on hybrid resources, based on the experimental cases described in Section 6.1 and the algorithms described above, we adjusted the flexibility parameters of the first five satellites of the nine total satellites. The maximum pitch angle and maximum roll angle were set to 0° and 0°, respectively. By adjusting the parameters, hybrid resources, including AEOSs and CEOSs, could be formed.

Based on the hybrid resources, the three algorithms were compared. As shown in Figure 19a, the objective function of the proposed algorithm was superior to the ISDR and TMBSR-DES algorithms, with values 25.46% and 14.46% higher on average, respectively. Accordingly, as shown in Figure 19b, the scheduled task value with the proposed algorithm was higher than those with the other two algorithms. Therein, the scheduled task value of the AEOSs was increased by 25.76% and 24.66% compared to the ISDR and TMBSR-DES algorithms on average, respectively, and the scheduled task value of the CEOSs increased by 25.25% and 6.54% on average, respectively. In terms of the scheduling capability for emergency tasks, as illustrated in Figure 19c, the scheduled emergency task value with the proposed algorithm was 2.19% and 1.47% higher than those with the ISDR and TMBSR-DES algorithms on average, respectively. Furthermore, the proposed algorithm produced a smaller disturbance measure based on the initial scheme, as shown in Figure 19d, and the disturbance measures for both the AEOS and CEOS schemes were generally smaller than those with the other two algorithms. Therefore, the proposed algorithm could complete the scheduling for the hybrid resources of AEOSs and CEOSs and produce better results.

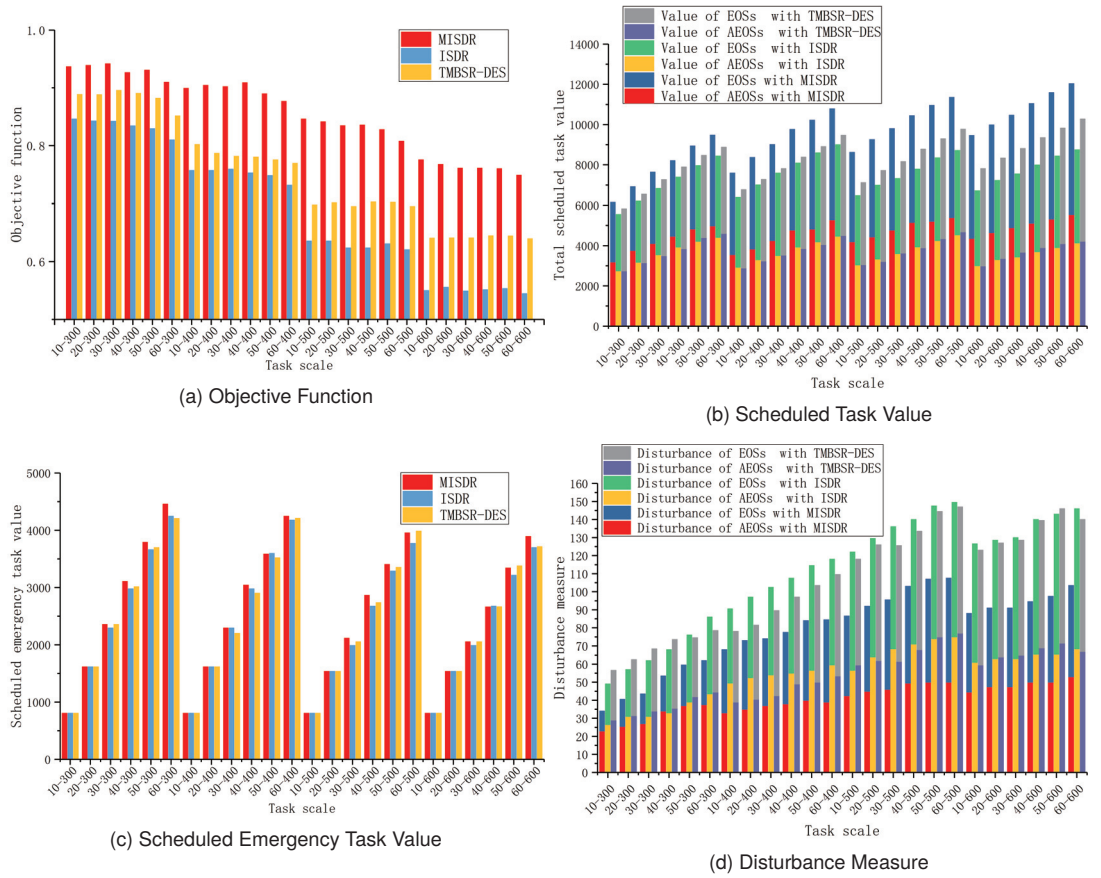

(a) Objective Function

(b) Scheduled Task Value

(c) Scheduled Emergency Task Value

(d) Disturbance Measure

Figure 18 Experimental Results for the Hybrid Resources

7. Conclusion and Future Work

In this paper, based on the high flexibilities of AEOSs and the short deadline and high value of emergency tasks, we studied AEOS scheduling for emergency tasks. First, we developed a novel time window division method to convert a VPVTW to multiple VTWs. Second, a more accurate model for AEOS scheduling was designed, including not only the general limitations of the data transmission time, turn-on time, turn-off time, storage, and energy, but also the limitations of the roll time, pitch time, and attitude stability time for AEOSs and the deadline for emergency tasks. To solve this model, we proposed the MISDR algorithm based on merging insertion, direct insertion, shifting insertion, deletion insertion, and reinsertion strategies to find a better solution. Moreover, we conducted multiple experiments, and the results indicated that the proposed algorithm could effectively improve the efficiency of AEOS scheduling for emergency tasks and meet the users' requests. The final experimental results showed that the proposed algorithm could support the scheduling for the hybrid resources of AEOSs and CEOSs.

There are a few open issues to be addressed in our future studies. First, the satellite resource capability model that can match the most suitable satellite resource set to the task set must be studied urgently. Second, further work on AEOS scheduling for regional emergency tasks is necessary. Finally, the scheduling for satellite and UAV collaboration is a new trend that should be studied in the future.

Acknowledgments

We would like to thank the anonymous reviewers for their constructive and detailed feedback

that substantially improved the paper. This work was supported by the National Natural Science Foundation of China under Grant Nos. 72071064 and 71521001.

Endnotes

[1] The left panel illustrates that the maneuver time between the tasks t_2 and t_3 is not satisfied, and thus, the task t_3 cannot be executed. The right panel illustrates that the AEOS can lengthen the visible time window of the task so that the observation start time of the task t_2 can be advanced to facilitate the execution of the task t_3.

References

Baek SW, Han SM, Cho KR, Lee DW, Yang JS, Bainum PM, Kim HD (2011). Development of a scheduling algorithm and GUI for autonomous satellite missions. *Acta Astronautica* 68(7): 1396-1402.

Bianchessi N, Cordeau JF, Desrosiers J, Laporte G, Raymond V (2007). A heuristic for the multi-satellite, multi-orbit and multi-user management of Earth observation satellites. *European Journal of Operational Research* 177(2): 750-762.

Bunkheila F, Ortore E, Circi C (2016). A new algorithm for agile satellite-based acquisition operations. *Acta Astronautica* 123:121-128.

Chen H, Wu J, Shi W, Li J, Zhong Z (2016). Coordinate scheduling approach for EDS observation tasks and data transmission jobs. *Journal of Systems Engineering and Electronics* 27(4): 822-835.

Cordeau JF, Laporte G (2005). Maximizing the value of an Earth observation satellite orbit. *Journal of the Operational Research Society* 56(8): 962-968.

Cui K, Xiang J, Zhang Y (2018). Mission planning optimization of video satellite for ground multi-object staring imaging. *Advances in Space Research* 61(6): 1476-1489.

Du B, Li S, She Y, Li W, Liao H, Wang H (2018). Area targets observation mission planning of agile satellite considering the drift angle constraint. *Journal of Astronomical Telescopes, Instruments, and Systems* 4(4): 047002.

Guo H, Zhu J, Ma M, Qiu D (2012). Observing scheme adjustment method for agile imaging satellites to achieve environment dynamic monitoring. *Research Journal of Chemistry and Environment* 16: 76-81.

Habet D, Vasquez M, Vimont Y (2010). Bounding the optimum for the problem of scheduling the photographs of an agile Earth observing satellite. *Computational Optimization and Applications* 47(2): 307-333.

Hao H, Jiang W, Li Y (2014). Improved algorithms to plan missions for agile Earth observation satellites. *Systems Engineering and Electronics* 25(5): 811-821.

Hall N, Magazine M (1994). Maximizing the value of a space mission. *European Journal of Operational Research* 78(2): 224-241.

He L, Liu X, Chen Y, Xing L, Liu K (2019). Hierarchical scheduling for real-time agile satellite task scheduling in a dynamic environment. *Advances in Space Research* 63(2): 897-912.

He L, Liu X, Laporte G, Chen Y, Chen Y (2018). An improved adaptive large neighborhood search algorithm for multiple agile satellites scheduling. *Computers & Operations Research* 100(Dec): 12-25.

He Y, Chen Y, Lu J, Chen C, Wu G (2019). Scheduling multiple agile Earth observation satellites with an edge computing framework and a constructive heuristic algorithm. *Journal of Systems Architecture* 95: 55-66.

Lemaître M, Verfaillie G, Jouhaud F, Lachiver J, Bataille N (2002). Selecting and scheduling observations of agile satellites. *Aerospace Science and Technology* 6(5): 367-381.

Li G, Xing L, Chen Y (2017). A hybrid online scheduling mechanism with revision and progressive techniques for autonomous Earth observation satellite. *Acta Astronautica* 140: 308-321.

Li Z, Li X (2019). A multi-objective binary-encoding differential evolution algorithm for proactive scheduling of agile earth observation satellites. *Advances in Space Research* 63(10): 3258-3269.

Liu S, Hodgson ME (2016). Satellite image collection modeling for large area hazard emergency response. *ISPRS Journal of Photogrammetry and Remote Sensing* 118: 13-21.

Liu X, Laporte G, Chen Y, He R (2017). An adaptive large neighborhood search metaheuristic for agile satellite scheduling with time-dependent transition time. *Computers & Operations Research* 86(Oct): 41-53.

Mao T, Xu Z, Hou R, Peng M (2012). Efficient satellite scheduling based on improved vector evaluated genetic algorithm. *Journal of Networks* 7(3): 517-523.

Niu X, Tang H, Wu L (2018). Satellite scheduling of large areal tasks for rapid response to natural disaster using a multi-objective genetic algorithm. *International Journal of Disaster Risk Reduction* 28: 813-825.

Niu X, Tang H, Wu L, Deng R, Zhai X (2015). Imaging-duration embedded dynamic scheduling of Earth observation satellites for emergent events. *Mathematical Problems in Engineering* : 1-31.

Peng S, Chen H, Li J, Jing N (2017). Approximate path searching method for single-satellite observation and transmission task planning problem. *Mathematical Problems in Engineering* : 1-16.

Qiu D, He C, Liu J, Ma M (2013). A dynamic scheduling method of Earth-observing satellites by employing rolling horizon strategy. *The Scientific World Journal* : 1-11.

Roychowdhury S, Allen TT, Allen NB (2017). A genetic algorithm with an earliest due date encoding for scheduling automotive stamping operations. *Computers & Industrial Engineering* 105: 201-209.

Song B, Yao F, Chen Y, Chen Y, Chen Y (2018). A hybrid genetic algorithm for satellite image downlink scheduling problem. *Discrete Dynamics in Nature & Society* : 1-11.

Sun H, Xia W, Hu X, Xu C (2019). Earth observation satellite scheduling for emergency tasks. *Journal of Systems Engineering and Electronics* 30(5): 931-945.

Wang J, Zhu X, Qiu D, Yang L (2014). Dynamic scheduling for emergency tasks on distributed imaging satellites with task merging. *IEEE Transactions on Parallel and Distributed Systems* 25(9): 2275-2285.

Wang M C, Dai G, Vasile M (2014). Heuristic scheduling algorithm oriented dynamic tasks for imaging satellites. *Mathematical Problems in Engineering* : 1-11.

Wang P, Reinelt G, Gao P, Tan Y (2011). A model, a heuristic and a decision support system to solve the scheduling problem of an earth observing satellite constellation. *Computers & Industrial Engineering* 61(2): 322-335.

Wang S, Zhao L, Cheng J, Zhou J, Wang Y (2019). Task scheduling and attitude planning for agile Earth observation satellite with intensive tasks. *Aerospace Science and Technology* 90: 23-33.

Wu G, Ma M, Zhu J, Qiu D (2012). Multi-satellite observation integrated scheduling method oriented to emergency tasks and common tasks. *Journal of Systems Engineering and Electronics* 23(5): 723-733.

Xie P, Wang H, Chen Y, Wang P (2019). A heuristic algorithm based on temporal conflict network for agile Earth observing satellite scheduling problem. *IEEE Access*: 61024-61033.

Xu R, Chen H, Liang X, Wang H (2016). Priority-based constructive algorithms for scheduling agile earth observation satellites with total priority maximization. *Expert Systems with Applications* 51: 195-206.

Zhai X, Niu X, Tang H, Wu L, Shen Y (2015). Robust satellite scheduling approach for dynamic emergency tasks. *Mathematical Problems in Engineering*: 1-20.

Zhu X, Sim KM, Jiang J, Wang J, Chen C, Liu Z (2017). Agent-based dynamic scheduling for Earth-observing tasks on multiple airships in emergency. *IEEE Systems Journal* 10(2): 661-672.

Haiquan Sun received his B.S. degree from Hefei University of Technology in 2016. He is currently working for his Ph.D. degree in management science and engineering at Hefei University of Technology. His research interests include satellite intelligent scheduling and emergency task scheduling.

Wei Xia received his Ph.D. degree from Hefei University of Technology in 2014. Currently he is working in University of Technology as a lecturer. His research interests include satellite intelligent scheduling and controlling.

Zhilong Wang received his B.S. degree from Hefei University of Technology in 2017. He is currently working for his Ph.D. degree in management science and engineering at Hefei University of Technology. His research interests include satellite resource scheduling and neural network scheduling algorithm.

Xiaoxuan Hu received his B.S. degree and Ph.D. degree from Hefei University of Technology in 1999 and 2007, respectively. He is a professor at Hefei University of Technology. His research interests include satellite scheduling and UAV planning.